Lattice-gas model based on field mediators for immiscible fluids

L. O. E. dos Santos and P. C. Philippi*
LMPT, Mechanical Engineering Department, Federal University of Santa Catarina, Caixa Postal 476 Florianopolis, Santa Catarina 88040-900, Brazil

(Received 21 December 2000; published 1 April 2002)

A Boolean lattice-gas model based on field mediators is proposed for simulating the flow of immiscible fluids. The field mediators introduced here simulate long-range action, enabling the use of local rules in separation step and, by avoiding the optimization step, reduce computer processing time with respect to previous models. In addition, field *strength* and *interaction* distance is modeled by introducing distinct emission P_e and extinction P_a probabilities, for field mediators, enabling us to *control* interfacial tension and transition thickness. The model's microdynamics is fully described and macroscopic parameters are related to model's parameters after a Chapman-Enskog asymptotic expansion for the ensemble-average distributions. Simulation results are presented for several sample case studies, including the verification of Laplace's law, coalescence phenomenon, interaction of a pair of wetting and nonwetting fluids with solid surfaces, and droplet formation under the action of gravity. These results are compared with available data.

DOI: 10.1103/PhysRevE.65.046305 PACS number(s): 47.11.+j

I. INTRODUCTION

Lattice-gas automata (LGA) designate a large class of models whose main feature is the presence of a set of particles moving in a discrete space (a lattice). In Boolean models, a Boolean variable $n_i(\mathbf{X},T)$ is attributed to each site $\mathbf{X}$ at time step T, indicating the presence ($n_i=1$) or absence ($n_i=0$) of a fluid particle . For each time step, the dynamic evolution of the model is given in two steps. In the first step, designated as *collision step*, the state of site $\mathbf{X}$ is changed following collision rules conceived so as to preserve total mass and momentum of the site. In the second step, called *propagation step*, particles are propagated to the neighbor sites, in accordance with their direction at site $\mathbf{X}$ after collision step. The use of such models to study and simulate fluid dynamics was first introduced by Hardy, Pomeau, and Pazzis [1], in 1973, but it was only after 1986 that these models grew in increased importance due to the work of Frisch *et al.* [2,3]. These authors formally demonstrated that the dynamics of such models under certain conditions was described by the Navier-Stokes equations for incompressible flows, and could be used to simulate such flows.

Mixtures and diffusion processes were simulated by distinguishing different kinds (say ψ) of particles [4,5]. Most common models use two-bit Boolean variables (r_i,b_i) representing colored particles of identical mass, such as red ($\psi=r$) and blue ($\psi=b$) and diffusion coefficient can be related to collisions frequency between particles of different colors. Exclusion principle is maintained between r and b particles.

Long-range attraction between particles of the same kind promotes particles separation, being responsible for interfacial tension, which acts as a potential barrier at the interface between fluids. Boolean models for simulating immiscible fluids flow were, first, proposed by Rothman and Keller [6]. In this model, long-range attraction between particles of the same kind is modeled by modifying the collision step, introducing an additional *separation* step between particles of different kinds, based on the information of the populations at first neighbors of site $\mathbf{X}$, at step T, $\psi_j(\mathbf{X}+\mathbf{c}_i,T)$, $i=1,\ldots,b_m$, $j=0_1,\ldots,0_{br},\ 1,\ldots,b_m$, where ψ designates the kind of particle found at direction j of site $\mathbf{X}+\mathbf{c}_i$ and $0_1,\ldots,0_{br}$ is used for bit occupation when model allows b_r rest particles. Output site configuration is decided after a maximization step for the color flux in accordance with a color gradient at site $\mathbf{X}$.

Rothman and Keller's model is computer expensive when processing time needs are considered. Somers and Rem [7] and Chen and co-workers [8] proposed a two-bit local model, where the time-consuming neighbor survey of Rothman and Keller is avoided, by introducing colored holes. Colored holes are null-mass particles representing the memory of the kind of a given particle, and moves in the same direction that particle moved before collision. The state of a given site is represented by a two-bit Boolean variable $(f_i(\mathbf{X},T),n_i(\mathbf{X},T))$, where $f_i=1$ designates red and $f_i=0$ represents blue, $n_i=1$ represents a particle and $n_i=0$ represents a hole. In this way, in separation step, red (blue) particles are deviated to the direction from where red (blue) holes were originated, simulating *long-range attraction*, by using, only, *local* rules. This is achieved by maximizing color flux $\mathbf{q}=\Sigma_i(2f_i-1)n_i\mathbf{c}_i$ in accordance with hole flux $\mathbf{q}_H=\Sigma_i(2f_i-1)(1-n_i)\mathbf{c}_i$, at a given site $\mathbf{X}$.

In Somers and Rem and in Chen *et al.* models, the optimization step is also processor time consuming. In fact, in both models, optimization step requires choosing among 3^7 configurations, in two-dimensional simulations and among 3^{24} configurations, in three-dimensional simulations, for each site, at each time step. Due to this computational limitation, Somers and Rem model was, in fact, designed to perform simulations in two dimensions, only.

In addition, in Rothman and Keller model, interaction distance is fixed and equal to a single lattice unit and in the two last models, interaction range is related to the mean free path of the single-phase collision rules, being dependent on density. In these models, interaction range is thus a fixed quan-

*Email address: philippi@lmpt.ufsc.br

tity for a given density and cannot be independently managed. A deep discussion on the influence of interaction range on error formation in modeling immiscible fluids is presented in Boghosian and Coveney [9]. Following Boghosian and Koveney, this error is related to the ratio h/l between lattice unit h and interaction range l and can be made to scale subdominantly to terms that are usually neglected in Chapman-Enskog expansion, by increasing l with respect to h.

Field mediators are null-mass particles moving with light speed, introduced in electromagnetic theory for the quantum description of long-range fields. They were first introduced in LGA theory by Appert *et al.* [10] when modeling phase transition. In present paper, we introduce field mediators for simulating the flow of fluid mixtures presenting arbitrary miscibility, with the following, distinguishing, main features: (i) such as in Chen's model, present *field mediators* move with the greatest lattice speed, $c=1$, enabling the use of *local* rules in separation step, (ii) emission and interference of present field mediators follow distinct rules when compared with Chen's *memory mediators* (holes), enabling to *avoid* Chen's optimization step, (iii) field *strength* and interaction distance is simulated by introducing distinct emission P_e and extinction P_a probabilities, for field mediators, allowing to control interfacial tension and transition thickness and the degree of mixing between different fluids, and, finally, (iv) possibility of simulating fluids with different viscosity coefficients and with an independently managed species diffusion coefficient. These features were achieved by introducing a four-bit Boolean model, described in the following section.

II. MODEL

The state of a given site X at time T is given by a four-bit Boolean variable $(r_i(\mathbf{X},T),\ b_i(\mathbf{X},T),\ m_i^r(\mathbf{X},T),\ m_i^b(\mathbf{X},T))$ where r_i, b_i, m_i^r, and m_i^b designate, respectively, r particles, b particles, r mediators, and b mediators. Model allows simultaneous r_i and b_i bit occupation, but exclusion principle is maintained between particles of the same kind. Particles are considered to have the same, unitary, mass.

Microdynamics has the following steps:

(i) *Collision.* Collisions are responsible for mixing particles of different kinds, in the transition region, being related to binary species diffusion coefficient D_{rb}. Microdynamics equation relating postcollision Boolean variable ψ_i' to ψ_i can be written as

$$\psi_i'(\mathbf{X},T)-\psi_i(\mathbf{X},T)$$

$$=\omega_i^{\psi}(r_{01},\ldots,r_{0b_r},r_1,\ldots,r_{b_m},b_{01},\ldots,b_{0b_r},b_1,\ldots,b_{b_m})$$

$$\equiv\omega_i^{\psi}(r^*(\mathbf{X},T),b^*(\mathbf{X},T)) \tag{1}$$

where $\psi^*=(\psi_{00},\ldots,\psi_{0b_r},\psi_1,\ldots,\psi_{b_m})$ designates a precollision ψ particles configuration of site $\mathbf{X}$, at time T,$00,\ldots,0b_r$ is related to Boolean occupation for b_r allowable rest particles in a lattice with b_m directions. A Boolean variable with $2b_t$ bits, $b_t=b_r+b_m$, is used to designate an arbitrary particle state $s=(s_{01}^r,\ldots,s_{0b_r}^r,s_1^r,\ldots,s_{b_m}^r,s_{01}^b,\ldots,s_{0b_r}^b,s_1^b,\ldots,s_{b_m}^b)$ of the lattice model in a $[(b_r+1)2^{b_m}]^2$-dimensional $B_r\times B_b$ space (rest particles are undistinguishable). Collision operator,

$$\omega_i^{\psi}:\quad B_r\times B_b\rightarrow\{-1,0,1\} \tag{2}$$

$$(r^*,b^*)\rightarrow\omega_i^{\psi}(r^*,b^*) \tag{3}$$

$\forall\ i=00,\ldots,0b_r,\ 1,\ldots,b_m$, maps a 2^{2b}-dimensional space on the set $\{-1,0,1\}$, respectively, *eliminating*, *leaving unaltered*, or *adding* a particle of kind ψ to direction i. Collision term can be written as

$$\omega_i^{\psi}(r^*,b^*)=\sum_{s,s'}\alpha_{\xi}(s,s')(s_i^{\psi\prime}-s_i^{\psi})$$

$$\times\prod_j r_j^{s_j^r}(1-r_j)^{1-s_j^r}b_j^{s_j^b}(1-b_j)^{1-s_j^b}, \tag{4}$$

where $\alpha_{\xi}(s,s')$ is the transition matrix, $\xi=\xi(X,T)$ is a random variable attributed to site $\mathbf{X}$, at time T. Transition matrix must assure, mass and momentum conservation

$$\sum_i\ \omega_i^r=\sum_i\ \omega_i^b=0, \tag{5}$$

$$\sum_i\ c_i(\omega_i^r+\omega_i^b)=0 \tag{6}$$

in collisions. In addition, let $A(s,s')$ be the ensemble average of $A(s,s')=\langle\alpha_{\xi}(s,s')\rangle$. As usually, considering the set Ξ of the all possible ξ random values, transition matrices $\alpha_{\xi},\ \xi\in\Xi$, must be written so as to satisfy the conservation of probability and semidetailed balance condition

$$\sum_{s'}\ A(s,s')=\sum_s\ A(s,s')=1 \tag{7}$$

as sufficient conditions for satisfying the H theorem in describing irreversibility of diffusion processes.

(ii) *Interference with field mediators*. In this step, particles of kind ψ, at site $\mathbf{X}$, are subjected to long-range attraction from particles of the same kind. In present model, this is simulated locally, by inverting the momentum of each ψ particle when (a) it finds a ψ mediator in the same direction and (b) opposite direction is free from ψ particles. Defining $n_{\psi}=\Sigma_i\psi_i$ $(\psi=r,b)$ and $n=n_r+n_b$, this step is, only, performed when $0<(n_{\psi})/n<1$, assuring a null effect of long-range fields and preserving single fluid state equation inside each phase. Interference step can, thus be written as

$$\psi_i''=\psi_i'(\mathbf{X},T)+\zeta(\psi'^*(\mathbf{X},T),m^{\psi}*(\mathbf{X},T)), \tag{8}$$

where

$$\zeta(\psi'^{*}(\mathbf{X},T),m^{\psi*}(\mathbf{X},T))=\psi'_{-i}m^{\psi}_{-i}(1-\psi'_{i})-\psi'_{i}m^{\psi}_{i}(1-\psi'_{-i}) \tag{9}$$

and $-i=(i+b_m/2)(\mathrm{mod}\ b_m)$, $i=1,\ldots,b_m$.

(iii) *Emission of field mediators*. Considering an elementary volume ϑ located inside a mixture of two real gases, ϑ acts as an attractive center for ψ molecules when n_ψ/n is above some critical value $(n_\psi/n)_{cr}$, with a potential strength that depends on the kind of r-r, b-b and, consequently, r-b, interactions. In present LGA model, site X will be a source of ψ mediators when $(n_\psi/n)>(n_\psi/n)_{cr}$, with a given emission probability P_e that depends on particle-ψ concentration n_ψ/n on site X, at time T. Emission probability is, thus, related to potential strength in the transition region, giving the interfacial tension σ_{rb}. When $P_e=0$, independently of n_ψ/n, fluids r and b will mix without long-range field restriction. On the other extreme, $P_e=1$, $\forall n_\psi/n$, represents a mixture of two, ideally, immiscible fluids.

Emission step can be written as

$$m^{\psi\prime}_{i}=\begin{cases}1 \quad \text{when } \dfrac{n_\psi}{n}>\left(\dfrac{n_\psi}{n}\right)_{cr} \quad \text{and} \quad P\leqslant P_e & (10)\\ m^{\psi}_{i} \quad \text{otherwise,} & (11)\end{cases}$$

where P is a random variable $(0\leqslant P\leqslant 1)$ attributed to site $\mathbf{X}$, at time T. In this way, b mediators found at an attractive site for r particles are preserved, during emission step, allowing the site to propagate this information to its neighboring sites, in propagation step.

(iv) *Extinction of field mediators*. In addition to field strength, interaction length is an important parameter, contributing to transition layer thickness. In present model, interaction length is related to an extinction probability P_a. Thus, for a field mediator $m^{\psi}(\mathbf{X},T)$ to be annihilated two conditions are imposed: (a) $n_\psi(\mathbf{X},T)=0$ and (b) $P(\mathbf{X},T)\leqslant P_a$, $(0\leqslant P\leqslant 1)$. These conditions assure that a field mediator ψ will never be destroyed in the transition region although r mediators will be found inside b phase, trying to rescue r particles moved to b phase by collisions. After extinction step

$$m^{\psi\prime\prime}_{i}=\begin{cases}0 \quad \text{when} \quad n_\psi=0 \quad \text{and} \quad P\leqslant P_a & (12)\\ m^{\psi\prime}_{i} \quad \text{otherwise.} & (13)\end{cases}$$

(v) *Propagation*. In propagation, particles and mediators are propagated to next neighbors, in the same manner as in conventional LGA models

$$\psi_i(\mathbf{X}+\mathbf{c}_i,T+1)=\psi''_i(X,T), \tag{14}$$

$$m^{\psi}_{i}(\mathbf{X}+\mathbf{c}_i,T+1)=m^{\psi\prime\prime}_{i}(\mathbf{X},T). \tag{15}$$

(vi) *Boundary conditions*. Wetting and nonwetting properties of a pair of fluids with respect to solid surfaces are a macroscopic result of differential, long-range attraction between solid and fluid molecules. At equilibrium, this preferential attraction can be summarized by the formation of a well defined contact angle θ between fluid interface and the solid wall, which depends on the pair of fluids and on the solid surface.

In present model, preferential attraction of solid wall, with respect to a given fluid p, is simulated by reflecting back ψ mediators at boundary sites $\mathbf{X}_b$, with a given probability P_r, related to θ. Nonwetting fluid mediators at boundary sites are not reflected, being annihilated at these sites. This condition may be written as,

$$m^{\psi}_{i}(\mathbf{X}_b,T+1)=\begin{cases}m^{\psi\prime\prime}_{i}(\mathbf{X}_b,T) \quad \text{when} \quad P(\mathbf{X}_b,T)\leqslant P_r & (16)\\ 0 \quad \text{otherwise,} & (17)\end{cases}$$

$\forall i$, pointing outward the solid surface, when ψ is the wetting fluid with respect to solid surface and where P, $0\leqslant P\leqslant 1$, is a random variable attributed to site $\mathbf{X}_b$, at time T.

External forces: Forcing step

Forcing step is performed before collision step, above described.

Labeling by k the lattice direction parallel to external field direction, external forces g_ψ are simulated by reversing the momentum of particles r and b, located at direction $-k$ opposed to g_ψ, when direction, k, is free from particles of the same kind. Probability $P_{g,\psi}$ to this reversion, represents the force strength g_ψ on component ψ. Microdynamical equation describing *forcing step* can be written as

$$\psi'_k(\mathbf{X},T)=\begin{cases}\psi_{-k}(\mathbf{X},T)[1-\psi_k(\mathbf{X},T)] \quad \text{when} \quad P(\mathbf{X},T)\leqslant P_{g,\psi} & (18)\\ \psi_k \quad \text{otherwise,} & (19)\end{cases}$$

where $P(X,T)$ is a random variable attributed to site $\mathbf{X}$, at time T, $0\leqslant P\leqslant 1$.

At equilibrium, using ergodic hypothesis when considering the whole lattice domain, the mean effect of forcing step on ψ particles can be calculated by,

$$f_\psi=2P_{g,\psi}\frac{\langle n_\psi\rangle}{b_t}\left(1-\frac{\langle n_\psi\rangle}{b_t}\right)c_k, \tag{20}$$

which is the force, related to the momentum the $\langle n_\psi\rangle$ particles per site are expected to gain in direction k during a lattice time step.

III. ENSEMBLE AVERAGES AND MACROSCOPIC PARAMETERS

Considering $\Psi_i(\mathbf{X},T)=\langle\psi_i(\mathbf{X},T)\rangle$ to be the expected value of $\psi_i(\mathbf{X},T)$ in several realizations the evolution equation for Ψ_i may be written as

$$\Psi_i(\mathbf{X}+\mathbf{c}_i,T+1)-\Psi_i(\mathbf{X},T)=(\Delta\Psi_i)_{col}+(\Delta\Psi_i)_g+(\Delta\Psi_i)^{lr}_{r-r}, \tag{21}$$

where $(\Delta P_i)_{col}$ is the change of Ψ_i due to r-r and r-b collisions on point $\mathbf{X}$, at time T, $(\Delta\Psi_i)_g$ is the change of Ψ_i

promoted by an external field g, and $(\Delta\Psi_i)^{lr}_{r\text{-}r}$ is related to long-range attraction between r particles.

A. Collision term

Equation (4) gives, using molecular chaos assumption,

$$(\Delta\Psi_i)_{col}=\Omega_i^{\psi}(R^*,B^*)=\sum_{s,s'}A(s,s')(s_i^{\psi\prime}-s_i^{\psi}) \times\prod_j R_j^{s_j^r}(1-R_j)^{1-s_j^r}B_j^{s_j^b}(1-B_j)^{1-s_j^b} \quad (22)$$

where $\Omega_i=\langle\omega_i\rangle$ is the expected value of collision term ω_i, at $\mathbf{X},T$, giving the probability a state $N=[R_0,R_1,\ldots R_{b_m},B_0,B_1,\ldots B_{b_m}]$ has a transition to state $N'=[R_0',R_1',\ldots R_{b_m}',B_0',B_1',\ldots B_{b_m}']$.

A Chapman-Enskog expansion for $M\sim \mathrm{Kn}\ll 1$, is performed on Ψ_i around Ψ_i^0 taken as the equilibrium solution of Boltzmann's equation,

$$\Psi_i=\Psi_i^0+\mathrm{Kn}\,\Psi_i^1+\mathrm{Kn}^2\,\Psi_i^2+\cdots, \quad \Psi=R,B, \quad (23)$$

where Kn and M are, respectively, Knudsen and Mach numbers. This expansion induces the decomposition of Ω, written in its linearized form as

$$\Omega_i^{\psi}=\Omega_i^{\psi,0}(R^{0*},B^{0*})+\mathrm{Kn}\sum_k(\Lambda_{ik}^{\psi,r}R_k^1+\Lambda_{ik}^{\psi,b}B_k^1) +\cdots, \quad \psi=r,b, \quad (24)$$

where $\Omega_i^{\psi,0}(R^{0*},B^{0*})=0$ and

$$\Lambda_{ik}^{\psi,r}=\left(\frac{\partial\Omega_i^{\psi}}{\partial R_k}\right)_{(R^{0*},B^{0*})}, \quad \Lambda_{ik}^{\psi,b}=\left(\frac{\partial\Omega_i^{\psi}}{\partial B_k}\right)_{(R^{0*},B^{0*})}. \quad (25)$$

Collision term $\Lambda_{ik}^{r,r}$ is related to the probability a r particle situated at direction k affects R_i population and $\Lambda_{ik}^{r,b}$, to the probability a b particle, at k, affects this population. Considering $\aleph^r$ to be the space of distributions $\mathbf{R}=[R_0,R_1,\ldots R_{b_m}]$, $\mathbf{R}$: $\mathbb{R}^D\to\mathbb{R}^{b_m+1}$, collision operator $\Lambda^{r,r}$: $\aleph^r\to\aleph^r$ is related to transitions on r populations promoted by r-r collisions and $\Lambda^{r,b}$: $\aleph^b\to\aleph^r$ is related to transitions on r populations promoted by r-b collisions.

Collision operators $\Lambda^{r,r}$ *and* $\Lambda^{r,b}$ are linear transformations. Macroscopic properties of pure component r, are related to the eigenvalues of some eigenvectors, respectively, λ_0^r of $[-b_m,1,\ldots,1]$ related to the second viscosity coefficient and λ_Q^r of $[0,Q_{1,\alpha\beta},\ldots,Q_{b_m,\alpha\beta}]$, $\alpha,\beta=1,\ldots,D$, related to the first viscosity coefficient. Similar considerations apply to b component, considering b-b collisions. Binary species diffusion coefficient D_{rb} is related to the eigenvalue λ_D^{rb} of $[0,c_{1\alpha},\ldots,c_{b_m\alpha}]$, $\alpha=1,\ldots,D$, which are eigenvectors of cross-collision operator, with non-null eigenvalue. In fact, by momentum conservation of r particles in r-r collisions, $[0,c_{1\alpha},\ldots,c_{b_m\alpha}]$ belongs to the kernel of $\Lambda^{r,r}$: $\aleph^r\to\aleph^r$; however, as r particles momentum is not conserved in r-b collisions the α component velocity vector $[0,c_{1\alpha},\ldots,c_{b_m\alpha}]$ is an eigenvector of cross-collision term with a *non-null* eigenvalue λ_D^{rb}.

B. External forces

The change of Ψ_i promoted by an external field $\mathbf{g}$ directed along a given lattice direction labeled g is given by

$$(\Delta\Psi_i)_g=\Psi_g^{\psi}\Psi_{-i}(1-\Psi_i)\,\delta(i,g). \quad (26)$$

In this way, the flow of immiscible fluids with very *different physical* densities under *gravity action*, may be simulated by adjusting probabilities $P_{g,r}$ and $P_{g,b}$ related to external forces. In fact, in low M approximation, *lattice* variables ρ_r and ρ_b affect, only, physical parameters related to collision term and *hydrostatic pressures* inside phases r and b, when probabilities $P_{g,r}$ and $P_{g,b}$ are adjusted to produce the appropriate buoyancy forces related to different r and b *physical densities*. In this way, considering low Mach number incompressible approximation and restricting ourselves to low Reynolds flows, Chapman-Enskog expansion gives for pure phase ψ,

$$\rho_{\psi}\partial_t u_{\psi,\beta}=\rho_{\psi}\partial_{\alpha}[\nu_{\psi,1}(\partial_{\alpha}u_{\psi,\beta}+\partial_{\beta}u_{\psi,\alpha})]-\partial_{\beta}p_{\psi}+\rho_{\psi}g_{\psi,\beta}, \quad (27)$$

where $p_{\psi}=c_s^2\rho_{\psi}$ is the pressure of component ψ and

$$g_{\psi}=2P_{g,\psi}\left[\frac{1}{b_t}\left(1-\frac{\rho_{\psi}}{b_t}\right)\right]c_g, \quad (28)$$

with direction g, as above, pointing to the direction of $\mathbf{g}$.

Considering ρ_{ψ}' as a rescaled density, written in the manner to satisfy $\rho_{\psi}g_{\psi,\beta}=\rho_{\psi}(2P_{g,\psi}/b_t)(1-f_{\psi})c_{g,\beta}=\rho_{\psi}'g_{\beta}=\rho_{\psi}'(2P_g/b_t)c_{g,\beta}$, where

$$P_g=\frac{f_r(1-f_r)P_{g,r}+f_b(1-f_b)P_{g,b}}{f_r+f_b} \quad (29)$$

is related to the external force acting on the whole mixture, the following expression is obtained for ρ_{ψ}':

$$\rho_{\psi}'=\rho_{\psi}(1-f_{\psi})\frac{P_{g,\psi}}{P_g}. \quad (30)$$

Equation (27) is rewritten in the form

$$\partial_t v_{\psi,\beta}=\partial_{\alpha}[\nu_{\psi,1}(\partial_{\alpha}v_{\psi,\beta}+\partial_{\beta}v_{\psi,\alpha})]-\frac{\partial_{\beta}p_{\psi}}{\rho_{\psi}'}+g_{\beta}, \quad (31)$$

where $v_{\psi}=(\rho_{\psi}/\rho_{\psi}')u_{\psi}$. In this way, for low Reynolds flow, ρ_{ψ}' is to be interpreted as the *apparent* density of fluid ψ, when this fluid is under gravity action. Considering, e.g., water as fluid r and oil as fluid b, as lattice particles have all the same mass, using a higher inversion probability $P_{g,r}$ for lattice particles related to water phase with respect to oil, $P_{g,b}$, it is possible to simulate differential gravity action on

these fluids. This is traduced by an *apparent* density ratio between lattice *r* and *b* lattice particles, equal to

$$r=\frac{\rho_r'}{\rho_b'}. \tag{32}$$

In the same way, in rescaled variables, $\mathbf{v}_\psi$ and $\mathbf{u}_\psi$ will be only identical when (i) physical densities of fluids *r* and *b* are equal and/or (ii) in absence of gravity.

C. Long-range factor

Considering Eq. (9) with $\psi=r$, describing the microdynamics at interference step, long range *r*-*r* attraction changes R_i by

$$(\Delta R_i)^{lr}_{r\text{-}r}=\langle\zeta\rangle=R_{-i}M^r_{-i}(1-R_i)-R_iM^r_i(1-R_{-i}), \tag{33}$$

where M^r_i is the probability of finding a *r* mediator on site *X*, at time *T*.

Calling $n_r/n=\omega_r$, $\omega_r(\mathbf{X},T)\equiv\omega_{r,0}$, $\omega_r(\mathbf{X}-\mathbf{c}_i,T-1)\equiv\omega_{r,-1}$, $\omega_r(\mathbf{X}-2\mathbf{c}_i,T-2)\equiv\omega_{r,-2}$ and so on, using the Heaviside function,

$$H(x-x_0)=0 \quad \text{for} \quad x<x_0, \tag{34}$$

$$H(x-x_0)=1 \quad \text{for} \quad x\geqslant x_0, \tag{35}$$

and noting $H^r_{-\tau}\equiv H(\omega_{r,-\tau}-\omega_r^*)$ and $H^{rb}_{-\tau}\equiv H(\omega_{b,-\tau}-1)$, annihilation probability of red particles will be given by

$$P^r_{ann}(\mathbf{X},T)=H(\omega_{b,o}-1)P_a=H^{rb}_0P_a \tag{36}$$

meaning that a *r* mediator to be annihilated must be in a pure *b* site and with probability P_a.

In this manner probability M^r_i can be written as a downward series,

$$\begin{aligned}M^r_i(\mathbf{X},T)=&H^r_{-1}P_e+H^r_{-2}P_e(1-H^r_{-1})(1-H^{rb}_{-1}P_a)\\&+H^r_{-3}P_e(1-H^r_{-1})(1-H^r_{-2})(1-H^{rb}_{-1}P_a)\\&\times(1-H^{rb}_{-2}P_a)+\cdots.\end{aligned} \tag{37}$$

The first two terms of this series are based on the fact that a *r* mediator will be found in *i* direction of site $\mathbf{X}$ at time *T*, if (a) it was produced on site $\mathbf{X}-\mathbf{c}_i$, at time $T-1$, with probability $H^r_{-1}P_e$, or when $\omega_{r,-1}<\omega_r^*$, (b) it has been produced at time $T-2$ and propagated from site $\mathbf{X}-2\mathbf{c}_i$ and not annihilated on site $\mathbf{X}-\mathbf{c}_i$. In this way, in equilibrium, considering, e.g., four sites numbered 1–4, inside the transition region, aligned in accordance with direction *i* and such that $\omega_{r,2}=\omega_{r,3}=\omega_{r,4}=0$, excepting for site 1 where $\omega_{r,1}\geqslant\omega_r^*$, the probability of finding a *r* mediator on site 4 will be given by the last term in above equation, i.e.,

$$P_e(1-H^{rb}_{-1}P_a)(1-H^{rb}_{-2}P_a)$$

meaning that a *r* mediator to be found on site 4 with, only, blue particles, it must be produced on site 1, with a predominantly number of *r* particles and not annihilated on sites 2 and 3.

When sites 2 and 3 are such that $\omega_{r,2}\neq 0$ *and* $\omega_{r,3}\neq 0$, this probability reduces to P_e since, in present model, *r* mediators are only annihilated on pure *b* phase.

IV. SIMULATION RESULTS

All simulations were performed on a face centered hypercubic (FCHC) lattice, with 24 degrees of freedom [11]. Considering computer resident memory requirements, a simplified collision table was used, replacing the 2^{48} bits complete table. In fact, complete collision table would require 200 terabytes of resident memory. In this way, in the collision step, a single fluid 2^{24} bits collision table is successively used, for particles *r* and *b*, respectively, followed by a random recoloring step. Very simple emission rules were chosen, by considering $(n_\psi/n)_{cr}=0.5$, $P_e=1$ and $P_a=0.5$. For two-dimensional simulations, a projection of FCHC lattice, was used, with four degrees of freedom attributed to each main axis, as a requirement for preserving fluid isotropy. For all presented results, initial conditions were chosen, by considering spatial average as around 9.6.

A. Laplace's law

Simulation started by placing an *r* cubic droplet, with a linear size of 20 lattice units, inside a 60^3, *b* domain with periodic conditions at outer boundaries and in the absence of gravity. Time averages were performed at each 10 time steps and final configuration is the average of 1000 time steps. Figure 1 shows simulation results in a sequence from initial condition to the final one, after 6000 time steps, showing a perfect spherical droplet. In fact, spherical form was an expected and physically consistent simulation result, as a consequence of long-range attraction between *r* particles.

In present problem, Laplace's law predicts a linear dependence between pressure drop and droplet radius, at equilibrium

$$\Delta p=\frac{(D-1)\sigma_{rb}}{R}, \tag{38}$$

where *D* is the Euclidean dimension of the space. Figure 2 shows $\Delta p=p_r-p_b$ plotted against $1/R$ for ten simulations, and the best straight line that considers the ten simulation results and cross the origin. Simulation domain was chosen as great enough to avoid boundary influence on simulation results (from 100×100, for simulating the small droplets to 300×300, for simulating the largest ones). Presented results are the average of 2×10^5 time steps for each radius. Pressure inside each phase is obtained by using single-fluid state equation $p=c_s^2\rho$, where c_s is the sound speed in FCHC lattice. Agreement with Laplace's law is quite good, giving the interfacial tension σ_{rb} this particular immiscible lattice-gas (ILG) model is intended to represent, in lattice units.

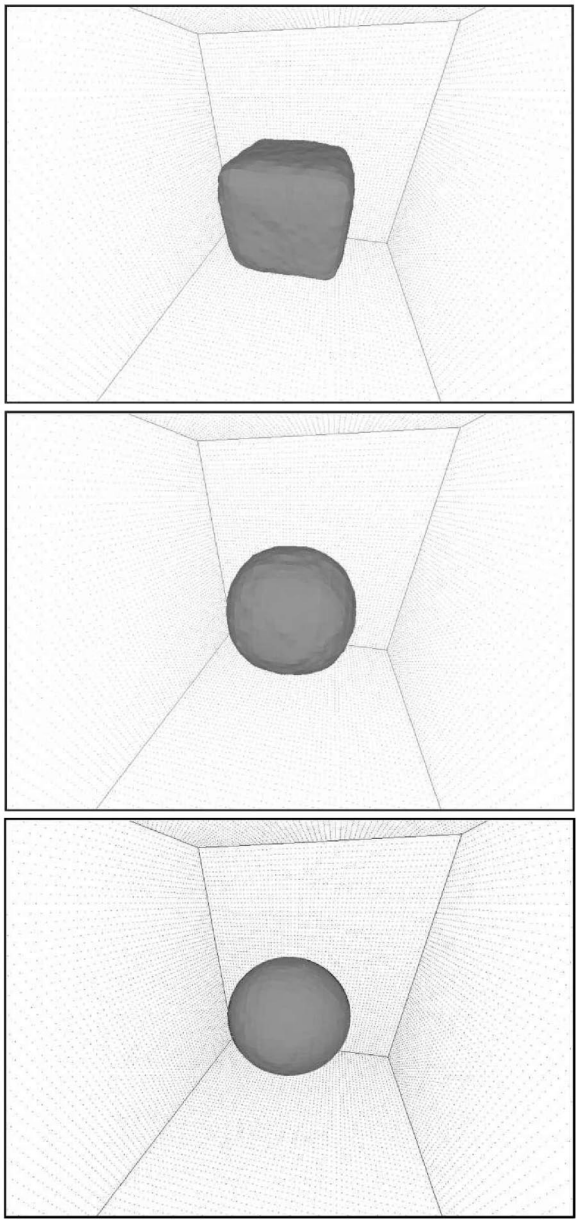

FIG. 1. Evolution from a cubic droplet left alone without any force field.

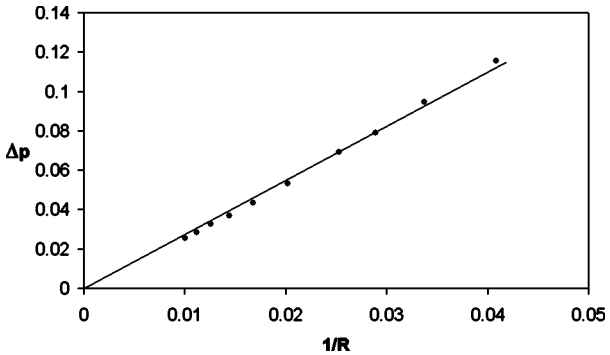

FIG. 2. Pressure difference inside and outside of a circular bubble as a function of the inverse of the radius (Laplace's law).

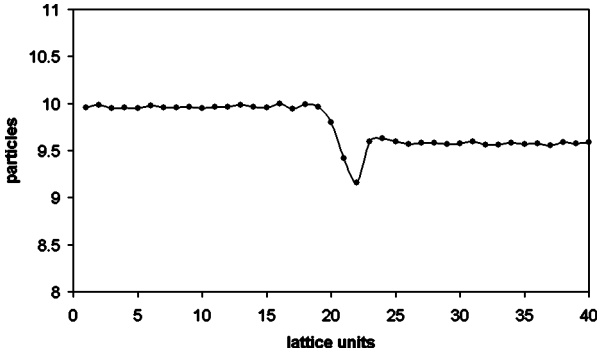

FIG. 3. Density variation across the interface of a circular bubble.

Figure 3 shows the spatial change of total density ρ, $\rho=\rho_r+\rho_b$. Total density has an abrupt decay from ρ_r, in the layer between 20 and 30 lattice units, being reestablished to ρ_b after the transition region. In this layer, simulation gives a sharp decay of ρ, in consequence of r and b particles separation, promoted by the strong interaction between particles and their respective field mediators. In real interfacial phenomena, this layer has a very small thickness related to interaction length of long-range forces. In present simulation, measuring unit for interaction length is the length scale $h=L/N$, where L is a characteristic length of the physical domain to be simulated and N is the number of lattice sites along L. In this way, as it was to be expected, although simulation results, correctly pictures the main physical aspects of interfacial phenomena, quantitative results related to distances h must be considered with care.

B. Momentum conservation

In present model, momentum is not locally conserved when particles are reversed due to field mediators action. Nevertheless, from a global point of view, it is expected that the effect of long-range forces will be zero when considering the total momentum of an isolated system of particles. Several simulations were performed, confirming this conjecture. Figure 4 shows the variation of x component of total momentum (Δmx) of a cubic domain with 50^3 lattice sites, taken as a cell in the domain problem of Fig. 1, after equilibrium was

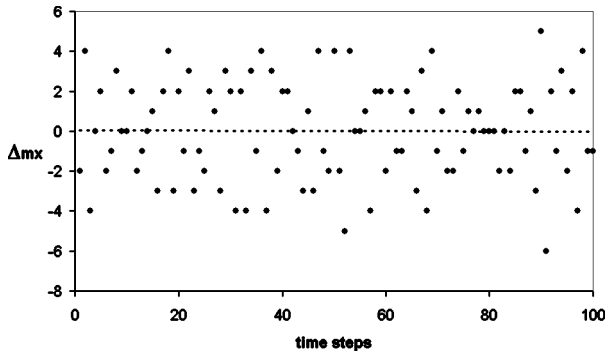

FIG. 4. Total momentum variation Δmx inside a cubic domain filled with immiscible fluids.

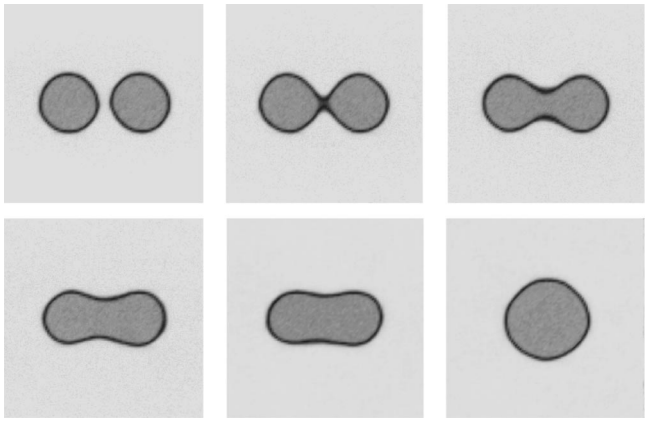

FIG. 5. Simulation of coalescence process between two circular bubbles.

reached. Although Δmx has time fluctuations due to the intrinsic nature of the model, its average value is zero as it was to be expected.

C. Coalescence

When two droplets r are put very closely, long-range fields arising from one of the droplets attract molecules belonging to the second droplet, giving rise to coalescence. Coalescence can be, physically, explained by considering the competition between: (i) dispersion of r molecules belonging to the surface of first droplet promoted by r-b collisions and (ii) long-range attraction from the second droplet. This is a very difficult interfacial phenomenon, which can, only, be fully described, in the molecular scale, related to interaction length of long-range forces In present work, coalescence phenomenon was simulated by the action of mediators, in the manner described in Sec. II. Simulation domain is 250^2 and each droplet has a radius of 25 lattice units. As depicted in Fig. 5, limiting ourselves to qualitative aspects and considering the physical limitations imposed by model's simplicity, simulation gave, nevertheless, an, apparently, correct picture of coalescence phenomenon.

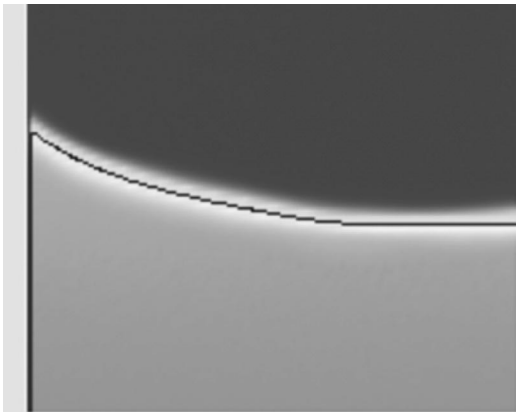

FIG. 6. Interaction between a pair of wetting and nonwetting fluids with a solid surface.

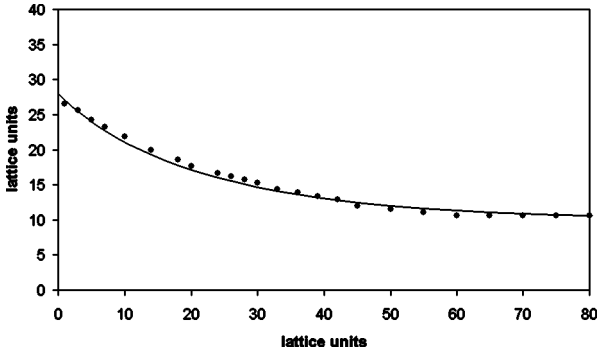

FIG. 7. Comparison between theoretical and simulated results of the shape a curve formed by a pair of wetting and nonwetting fluids near a solid surface.

D. Interaction between a pair of wetting and nonwetting fluids with a solid surface

Figure 6 shows simulation results for the equilibrium solution, $y(x)$, giving the interface geometrical configuration for a pair of a wetting (r) and a nonwetting (b) fluids in contact with a solid surface. Simulation domain has 300^2 sites and simulation results are the average of 2×10^5 time steps. Ordinate y gives the wetting fluid raise for each interfacial point at a distance x from the solid surface, in lattice units. Gravity action is simulated in accordance with Sec. II A, reversing the momentum of r and b particles with a given probability P_g. A theoretical expression for the interfacial shape $y(x)$, in equilibrium, is given in Batchelor [12], in terms of contact angle θ interfacial tension σ_{rb}, and gravity acceleration g. Figure 7 compares simulation with theoretical results of $y(x)$. Interfacial tension σ_{rb} was obtained by direct simulation of Laplace's law (subsection A), gravity acceleration is given by Eq. (28) and contact angle was directly measured on Fig. 6. Comparison shows a very good agreement between theoretical and simulated results for interfacial shape $y(x)$.

E. Droplet formation from a dropper under the action of gravity

Although very interesting from a physical point of view, droplet formation from a dropper is a very difficult problem, when we consider classical discrete methods of fluid mechanics. Droplet formation is pictured in Fig. 8 (from Adanson [13]) showing a sequence of drawings based on high speed photographs.

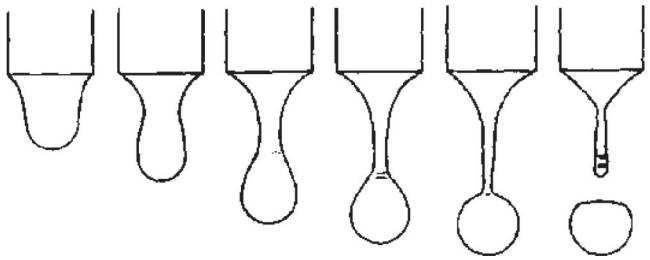

FIG. 8. Photograph of a droplet, from Adamson [13] (reprinted with permission of John Wiley & Sons, Inc.).

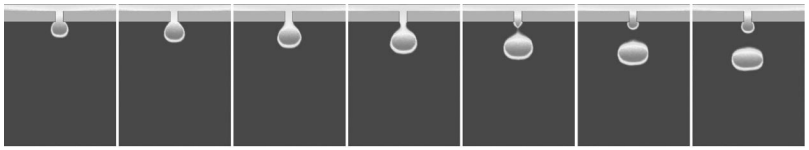

FIG. 9. Simulation of the growth and detachment of a droplet due to gravity.

From a macroscopic point of view droplet's shape time evolution is linked to the competition it is subjected between gravity action, viscosity of the droplet fluid and interfacial tension. In this way, interfacial forces hold the droplet until breakoff, as droplet weight increases. Breakoff starts with the development of a throat, which becomes thinner in time and from where droplet fluid is pulled downward against the droplet and redistributed horizontally by viscous forces, giving an almost ellipsoidal shape to the falling droplet, with a major axis oriented along horizontal direction.

From a microscopic point of view, during the first moments of droplet fall, *r* particles at droplet surface are subjected to long-range forces from *r* phase inside the dropper, maintaining the integrity of *r* phase in despite of gravity action. Droplet breakoff starts when combined action of gravity and downward long-range attraction from the created droplet increases with respect to upward long-range attraction from *r* phase inside the dropper, giving raise to the formation of droplet throat. During and after breakoff, *r* particles in the throat are pulled against the droplet, where these particles are redistributed inside the droplet by *r*-*r* collisions (related to the viscosity of droplet fluid).

Figure 9 shows a sequence of simulation results, considered as time averages for each 200 time steps, using present field-mediators model, on a 200×300 simulation domain. Comparison of Figs. 8 and 9 shows a very good qualitative agreement between simulation and experimental results.

V. CONCLUSIONS

Although greatly simplifying the microdynamics and enabling Boolean arithmetic, exclusion principle of Boolean models leads to lattice effects, which become of increased importance for lattices with a small number of degrees of freedom. Reducing particles occupation on lattice sites can reduce these effects, but increases processing-time and noise effects. On the other way, the number of degrees of freedom is limited to computer storage capacity, which needs increase by a factor of two for each unitary increment in the lattice degrees of freedom. Considering these limitations, interfacial phenomena present in the flow of immiscible fluids represent a field of great interest where lattice gas automata concepts appear to be very suitable for explaining complex macroscopic effects, based on simple models of fluid behavior at molecular level. In this paper a new Boolean model based on a four-bit variable for each lattice direction was presented for simulating the flow of immiscible fluids. Field mediators were introduced for representing the action of long-range fields, but with an interference step described by local rules. In addition, emission and extinction probabilities enable to control interfacial tension and transition thickness. Taking the above limitations into account and considering its simplicity, simulation results, apparently, confirm the adequacy of presently proposed model to study physical phenomena related to the flow of immiscible fluids.

ACKNOWLEDGMENTS

This work was supported by CNPq (Brazilian Council of Scientific and Technological Development) and CTPETRO (Scientific and Technological Program for Petroleum and Natural Gas). The authors thank Sávio Leandro Bertoli for very helpful discussions.

[1] J. Hardy, Y. Pomeau, and O. de Pazzis, J. Math. Phys. **14**, 1746 (1973).
[2] U. Frisch, B. Hasslacher, and Y. Pomeau, Phys. Rev. Lett. **56**, 1505 (1986).
[3] U. Frisch, D. d'Humières, B. Hasslacher, P. Lallemand, Y. Pomeau, and J. Rivet, Complex Syst. **1**, 649 (1987).
[4] H. Chen and W. H. Matthaeus, Phys. Fluids **30**, 1235 (1987).
[5] C. Burges and S. Zaleski, Complex Syst. **1**, 31 (1987).
[6] D. H. Rothman and J. Keller, J. Stat. Phys. **52**, 1119 (1988).
[7] J. A. Somers and P. C. Rem, Physica D **47**, 39 (1991).
[8] S. Chen, G. Doolen, K. Eggert, D. Grunau, and E. Loh, Phys. Rev. A **43**, 7053 (1991).
[9] B. M. Boghosian and P. V. Coveney, Comput. Phys. Commun. **129**, 46 (2000).
[10] C. Appert, D. d'Humières, V. Pot, and S. Zaleski, Transp. Theory Stat. Phys. **23**, 107 (1993).
[11] D. d'Humières, P. Lallemand, and U. Frisch, Europhys. Lett. **2**, 291 (1986).
[12] G. K. Batchelor, *An Introduction to Fluid Dynamics* (Cambridge University Press, Cambridge, England, 1967).
[13] A. Adamson, *Physical Chemistry of Surfaces*, 5th ed. (Wiley, New York, 1990).